[1]*Alkali Halide Vapors: Structure; Spectra and Reaction Dynamics*, edited by P. Davidovits and D. L. McFadden (Academic, New York, 1979).
[2]C. M. Rosenblatt, *High Temperature Science: Future Needs and Anticipated Developments* (National Academy of Sciences, Washington, D. C., 1979), p. 23.
[3]M. Blander, in Ref. 1, p. 6.
[4]T. P. Martin, Phys. Rev. B 15, 4071 (1977).
[5]J. Berkowitz, in Ref. 1, p. 155–188.
[6]J. Berkowitz, in *Electron Spectroscopy: Theory, Applications and Techniques*, edited by C. R. Brundle and A. D. Baker (Academic, New York, 1977), Vol. 1, p. 355–433.
[7]M. Szymomski, H. Overeijnder, and A. E. DeVries, Rad. Effects 36, 189 (1978).
[8]F. Honda, G. M. Lancaster, Y. Fukuda, and J. W. Rabalais, J. Chem. Phys. 69, 4931 (1978).
[9]D. O. Welch, O. W. Lazareth, G. J. Dienes, and R. D. Hatcher, J. Chem. Phys. 68, 2159 (1978).
[10]T. P. Martin, J. Chem. Phys. 72, 3506 (1980).
[11]R. J. Colton, J. E. Campana, T. M. Barlak, J. J. DeCorpo, and J. R. Wyatt, Rev. Sci. Instrum. 51, 1685 (1980).
[12]T. M. Barlak, J. E. Campana, R. J. Colton, J. J. DeCorpo, and J. R. Wyatt, to be published.
[13]R. Buhl and A. Preisinger, Surf. Sci. 47, 344 (1975).
[14]M. G. Dowsett, R. M. King, and E. H. C. Parker, Surf. Sci. 71, 541 (1978).
[15]G. Blaise and A. Nourtier, Surf. Sci. 90, 495 (1979).
[16]N. Winograd and B. J. Garrison, Acc. Chem. Res. 13, 406 (1980).
[17]T. M. Barlak, J. R. Wyatt, R. J. Colton, J. J. DeCorpo, and J. E. Campana, unpublished results.
[18]J. E. Campana, unpublished results.
[19]G. Staudenmaier, W. O. Hopper, and H. Liebl, Int. J. Mass. Spectrom. Ion Phys. 21, 103 (1976).
[20]J. E. Campana, J. J. DeCorpo, J. R. Wyatt, and R. J. Colton, unpublished results.
[21]E. Seitz, *The Modern Theory of Solids* (McGraw-Hill, New York, 1940), p. 76–98.
[22]S. Kirkpatrick, in *Ill-Condensed Matter*, edited by R. Balian, R. Maynard, and G. Toulouse (North-Holland, Amsterdam, 1979), p. 321–403, and references therein.
[23]M. Yamada, Phys. Z. 24, 364 (1923), and 25, 52 (1924).
[24]C. Kittel, *Introduction to Solid State Physics* (Wiley, New York, 1968), p. 20.
[25]T. P. Martin, J. Chem. Phys. 69, 2036 (1978).
[26]L. G. Christophorou, *Atomic and Molecular Radiation Physics* (Wiley-Interscience, New York, 1971), p. 521–553.
[27]P. T. Murray and J. W. Rabalais, J. Amer. Chem. Soc. 102, 1007 (1981).

Stability of Ablatively Accelerated Thin Foils

A. Raven,[a] H. Azechi, T. Yamanaka, and C. Yamanaka
Institute of Laser Engineering, Osaka University, Suita, Osaka 565, Japan
(Received 17 March 1981)

The stability of ablatively accelerated single-layer and multilayer thin foil targets has been studied by x-ray shadowgraphy and x-ray spectral analysis of the rear target surface. Results show the single-layer foil acceleration to be essentially stable with the disassembly being thermally dominated. An upper limit to Rayleigh-Taylor growth of 1.8 is determined compared to a classical value of 11. Evidence, though, of internal layer mixing in the multilayer target is seen.

PACS numbers: 52.35.Py, 52.55.Mg

One of the topics currently of interest to the field of laser-driven compression is the stability of the targets under ablative acceleration. Such instabilities may arise either from nonuniform laser irradiation or from hydrodynamic instabilities, of which the Rayleigh-Taylor (RT) instability is perhaps the best known. Such instabilities, if they occur, could seriously limit the performance of ablatively driven compression for all but the lowest-aspect-ratio targets. A number of theoretical studies related to this problem have been carried out[1,2] and some indirect indications of instability occurring have been seen in ablatively driven implosions.[3] However, to date the only direct evidence has been on the inner surface of electron-beam–imploded cylinders.[4] We present here the results of two experiments to examine the problem of target stability under ablative acceleration. The first involves observing the behavior of a single-layer accelerated target by x-ray backlighting. In contrast to previous optical shadowgraphy measurements[5] this technique allows the high-density target material to be studied. The use of foil acceleration re-

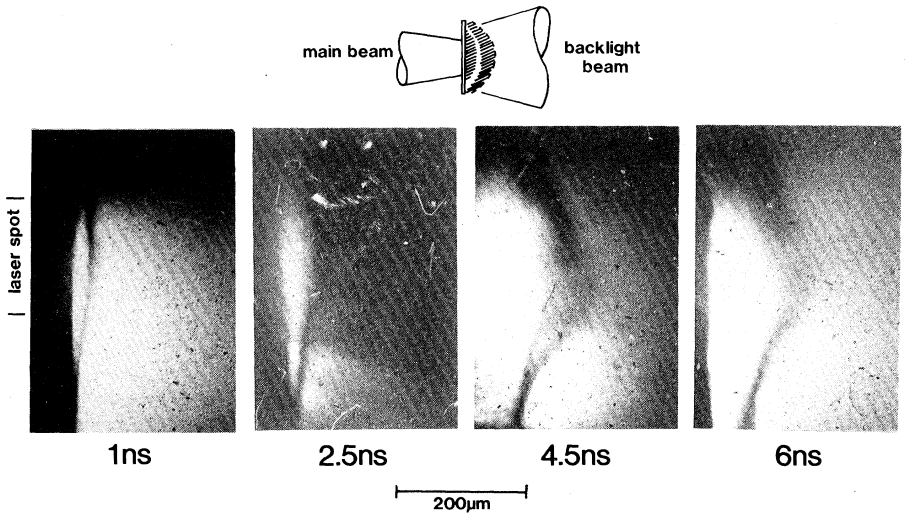

FIG. 1. Framing x-ray shadowgraphs of a 3-μm-thick Mylar foil irradiated at 3.6×10^{13} W/cm^2. The time delay between the peak of the main and backlighting pulses is shown below each image.

moves the problems involved with convergence in spherical shells but may introduce edge effects.[5] The second involves the diagnosis of the rear surface composition of a multilayer target after acceleration by using a low-energy probe beam to excite x-ray lines from the rear surface.

The experiment was carried out on the Gekko II two-beam laser system, the details of which can be found elsewhere.[6] For the backlighting studies, targets consisting of 1-mm-wide strips of 3-μm-thick Mylar and 12-μm-thick polyethylene were used. A 6-μm-thick Al foil was mounted coplanar with and at 2 mm separation from the Mylar foil to form the backlighting source. The Mylar strips were irradiated with an $f/5$ beam in a Gaussian pulse of 800 ps full width at half maximum and a focal spot size of 200×300 μm^2 (measured from the size of the x-ray emission region). The backlighting source was irradiated by an $f/1.2$ beam defocused to a spot size of 300 μm and delayed between 1 and 6 ns relative to the main beam. For all shots the main beam energy was 27 ± 3 J giving an intensity of $(3.6\pm0.4)\times10^{13}$ W/cm^2 on target. The backlighting energy was of the same order. The target was imaged by a 10-μm pinhole with a magnification of 10× and a filter of 25 μm Be.

A series of x-ray backlighting images of a 3-μm-thick foil is shown in Fig. 1. In these images the resolution along the laser beam axis is limited by the duration of the x-ray pulse to about 25 μm, but in the direction parallel to the target surface it is limited by the pinhole size to about 10 μm. The resolution parallel to the target surface is sufficient to resolve instabilities with wavelengths greater than 10 μm. Such wavelength instabilities are possible due to irradiation nonuniformity and filamentation,[7] both of which have wavelengths on the order of 10–20 μm.

Because of the time integration and the broad backlighting spectrum no attempt is made to derive mass distribution data but the following qualitative observations can be made. At the end of the acceleration phase (1 ns) the foil has been accelerated as a well behaved high-density layer over a region consistent with the focal spot size and with no visible deformations attributable to filamentation or laser nonuniformity (we estimate that less than 30% differential acceleration should be detectable). The smooth blending of the accelerated and unaccelerated regions is indicative of some smoothing of the rather sharp-edged focal spot profile which might be expected to have given a detached slug of accelerated material. At later times the central portion of the accelerated foil broadens and becomes of lower density although the outer regions remain well defined (the broadening of the upper edges in Fig. 1 is probably due to the softer x-ray spectrum at the edge of the backlight source).

In Fig. 2 we plot the position and image width of the foil as a function of time to obtain an estimate of the acceleration parameters. From the x-ray data we can estimate the mean foil velocity at 2.6×10^6 cm/s and an expansion velocity of 5

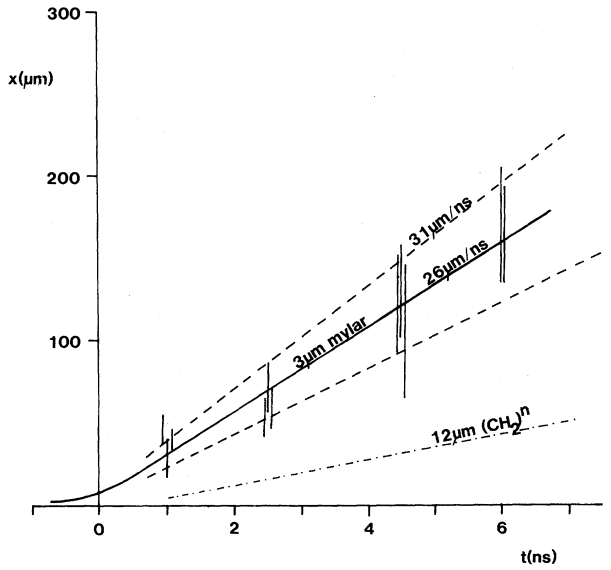

FIG. 2. Foil trajectory and expansion. Vertical bars mark the foil position and width derived from Fig. 1 and similar data. The solid and dotted lines show the best-fit trajectories for the center and surfaces of the foil, respectively.

$\times 10^5$ cm/s. Because of time integration and curvature effects this represents an upper limit on the expansion velocity. By assuming a suitable scaling for the ablation pressure with intensity ($P \propto I^{2/3}$) we can integrate up the equation of motion of the foil and fit the terminal velocity to the measured velocity. This gives an ablation pressure of 1.0 Mbar. This pressure is a factor of 5–10 lower than that measured by other means.[4,8] The edge effects may be playing some part but the spot size is little different from the 300-μm-diam targets used in Ref. 5. However, we will not address here the question of ablation pressure as it is only the foil acceleration that is important for stability estimates. That the pressure discrepancy is not related to the foil stability can be seen from the similar pressure of 0.8 Mbar obtained for the more stable 12-μm-thick foil.

Of importance to the stability question is the foil expansion. The measured upper limit on the foil expansion velocity is consistent with a thermal disassembly of the target for a preheat temperature of 3 eV. This temperature is lower than that of 8 eV reported for a 4-μm Al foil[9] at 10% of the intensity used here. There the preheat was attributed to x rays generated by the laser interaction, so that 3 eV is not unreasonable as Mylar is a much less efficient x-ray source than Al. Although the disassembly can be accounted for by target preheat, it also sets an upper limit on the RT growth. The linear and nonlinear phases of RT growth are well understood[10] although the transition is complex. For small γt, linear theory is valid and we can estimate the foil expansion velocity at the end of the acceleration as $d(\delta_0 e^{\gamma t})/dt$, i.e. $(\gamma t)e^{(\gamma t)} = v_{\exp} t/\delta_0$ where $v_{\exp}$ is the foil expansion velocity, t is the acceleration time, and δ_0 is the target surface finish (~0.5 μm at $\lambda = 3$ μm from secondary-emission monitor measurements). This then sets an upper limit on γt of 1.8 compared with a classical value of 11 calculated from the foil acceleration and under the assumption of a wavelength equal to the foil thickness.[2] Consistency between the measurement and the calculation would require a wavelength greater than 100 μm. This then implies either that γ is reduced below the classical value or that saturation of the growth occurs at a very early stage so that t is effectively reduced. We can estimate the time to saturation using the nonlinear theory.

In the nonlinear regime[10] the front surface falls freely in the frame of the accelerated foil. We assume that the front surface accelerates with the foil until the nonlinear phase is reached and then falls freely with a constant velocity v_{ff} in the laboratory frame. This two-step model will tend, if anything, to underestimate the time at which saturation occurs as it ignores any contribution to v_{ff} from the linear phase. This model gives the front surface velocity as $v_{ff} = at_s$ where a is the acceleration and t_s is the time at which saturation occurs. Since this gives a saturation time of the order of the pulse length, we are left with the conclusion that γ is reduced below the classical value by at least a factor of 6. Since the instability becomes nonlinear at amplitudes $\lesssim \Delta r$,[10] the foil thickness, we can independently estimate that $\delta_0 e^{\gamma t} \lesssim \Delta r$ or $\gamma t \lesssim 1.8$, confirming the linear-theory estimate.

One mechanism for reducing γ is viscosity effects. However, for classical viscosity,[11] the stabilization introduced at a 3-μm wavelength is small. Other mechanisms for stabilization in an ablative flow have been published[1] but will not be discussed here as no distinction can be made between them on the basis of this data.

These measurements have shown the absence of large-scale instabilities due to irradiation nonuniformities or filamentation, that small-scale instabilities are not dominant over thermal disassembly due to preheating, and that the RT

growth at the ablation front is below the classical value.

However, to check for mixing in multilayer accelerated foils we accelerated multilayer targets consisting of 4-mm-diam discs of either CH(2 μm)/Al(2 μm)/Si(1 μm) or Au(0.2 μm)/Al(0.7 μm)/Au(0.2 μm) sandwiches. The front layer (CH or Au) was irradiated under conditions similar to the Mylar foils, but the backlighting beam was reduced to 0.5 J energy and focused to a 50-μm spot centered on the accelerated region and delayed by 1 ns. This probe beam, which was a small perturbation on the foil for all except the lowest-energy shots, excited x-ray lines from the rear target surface to diagnose its composition after the acceleration. The x-ray spectrum was measured in the range 1–3 keV with a miniature time and space integrating thallium acid phthalate crystal spectrometer, with spatial resolution being provided by the small probe size. The target acceleration was varied by changing the main laser energy which could be varied independently of the backlight energy. Target acceleration was estimated by scaling the Mylar foil data. In Fig. 3 we plot the intensity of the Al $1s^2$-$1s2p$ line as a function of the estimated γt. Careful checks were made to ensure that front surface burnthrough was not responsible, and this was confirmed by the narrow lines compared with the broad lines emitted from an ablation plasma. Great care was necessary to avoid surface contamination by the debris from previous targets and targets were therefore mounted singly in the chamber. Careful alignment and the small probe area compared to the accelerated target rule out edge effects. From the Al/Si $1s^2$-$1s2p$ line ratio we estimate that peak mixing corresponds to an 18% ion density of Al for a probe plasma temperature of 370 eV. The temperature was estimated from the ratios of H- and He-like Si lines by the assumption of a simple coronal model[12] since the continuum was too weak to measure. However, errors in this temperature have only a small effect on the estimated mixing level (a change of 100 eV changes the mixing estimate by 4%). The diffusion velocity of Al through Si is estimated at 0.1 μm/ns and is essentially independent of the preheat temperature ($\propto T^{1/4}$). The most likely candidate for the mixing is RT instability at the CH/Al or Al/Au interfaces which, being in the interior of the target, would not be stabilized by the ablation process. However, further studies are necessary to clarify the cause of the mixing.

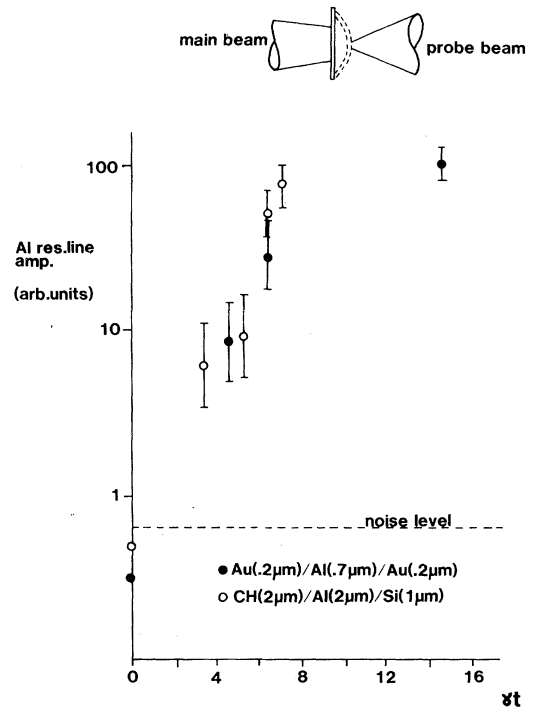

FIG. 3. Al resonance-line amplitude vs foil acceleration (estimated by scaling the data of Fig. 2 and by using $\lambda = \Delta r$) for multilayer targets. For the CH/Al/Si targets, 100 corresponds to 18% mixing.

In conclusion, we have demonstrated that thin foils can be accelerated without observable nonuniformities due to nonuniform illumination or filamentation. The disassembly of single-layer foils is consistent with the expected level of preheat and is not dominated by the RT instability as would be expected from classical arguments. The RT growth is reduced by at least a factor of 6 relative to the classical value. In multilayer targets mixing within the foil occurs up to a maximum level of 20% and may be due to instability at the layer interfaces within the target.

One of us (A. R.) would like to thank the Japan Society for the Promotion of Science for support under their Research Fellowship Program.

[a]Permanent address: Rutherford Laboratory, Chilton, Didcot, Oxon, United Kingdom.

[1]S. E. Bodner, Phys. Rev. Lett. 33, 761 (1974); J. D. Lindl and W. C. Mead, Phys. Rev. Lett. 34, 1273 (1975); R. L. McCrory and R. L. Morse, Phys. Fluids 19, 175 (1975); K. A. Brueckner, S. Jorna, and R. Janda, Phys. Fluids 22, 1841 (1979).

[2]R. L. McCrory, L. Montierth, R. L. Morse, and C. P. Verdon, Phys. Rev. Lett. 46, 336 (1981).
[3]M. H. Key *et al.*, Phys. Rev. Lett. 45, 1801 (1980).
[4]F. C. Perry, L. P. Mix, L. Baker, and A. J. Toepler, Bull. Am. Phys. Soc. 23, 854 (1978).
[5]B. H. Ripin *et al.*, Phys. Fluids 23, 1012 (1980).
[6]C. Yamanaka *et al.*, to be published.
[7]O. Willi and P. T. Rumsby, to be published.
[8]A. Gibson, Rutherford Laboratory Annual Report No. RL-80-026 (unpublished).
[9]E. A. McLean *et al.*, Phys. Rev. Lett. 45, 1246 (1980).
[10]B. J. Daly, Phys. Fluids 10, 297 (1967).
[11]L. Spitzer, *Physics of Fully Ionized Gases* (Interscience, New York, 1961).
[12]F. C. Young *et al.*, Appl. Phys. Lett. 30, 45 (1977).

Modified Korteweg–de Vries Equation for Propagating Double Layers in Plasmas

S. Torvén
Department of Plasma Physics, Royal Institute of Technology, S-10044 Stockholm 70, Sweden
(Received 3 June 1981)

A modified Korteweg–de Vries equation with a cubic nonlinearity is found to describe the time evolution of propagating double layers or electrostatic shocks. The asymptotic form of the solution is discussed for a monotonic initial profile. The profile may steepen and reach a steady state simultaneously as a number of solitary waves form behind the shock, resembling the time evolution of experimentally observed shock profiles.

PACS numbers: 52.35.Mw

The formation of double layers or electrostatic shocks in plasmas has been investigated,[1] but the significant mechanisms in different processes for double-layer formation are still unclear. When a potential drop and a localized electric field exist initially, the shock propagation for small amplitudes has been studied in double plasma devices,[2,3] and propagating one-dimensional ion acoustic shocks have also been investigated theoretically when the initial potential gradient is weak so that quasineutrality prevails.[4] In this paper the Poisson equation will be included in the analysis by assuming small shock amplitudes so that only first-order effects of nonlinearity and dispersion need to be considered. The ions are also assumed to have a vanishingly small temperature, and the motion is considered on the ion acoustic time scale so that the electron distribution function may be approximated by a steady-state distribution function. We shall find that a modified Korteweg–de Vries (MKdV) equation with a cubic nonlinearity describes the time evolution of double layers when the plasma on the high potential side has a population of trapped electrons, and some interesting properties of the asymptotic shock solution for large times will be derived.

Under the above assumptions the ion motion is determined by the equations

$$h_t+(hv)_x=0, \tag{1}$$

$$v_t+vv_x+\varphi_x=0, \tag{2}$$

$$\varphi_{xx}=h_e(\varphi)-h. \tag{3}$$

Here $h=n_i/n_0$, $h_e=n_e/n_0$, $v=v_i/(k_B T_e/m_i)^{1/2}$, and $\varphi=eV/k_B T_e$. The ion and electron number densities are denoted by n_i and n_e, v_i is the ion velocity, V the electric potential, T_e the electron temperature, k_B Boltzmann's constant, m_i the ion mass, and e the positive elementary charge. The coordinates are also normalized so that $x=x'/\lambda_D$ and $t=\omega_{pi}t'$, where x' and t' are the space and time coordinates, $\lambda_D=(\epsilon_0 k_B T_e/n_0 e^2)^{1/2}$, and $\omega_{pi}=(n_0 e^2/\epsilon_0 m_i)^{1/2}$.

First we investigate solutions describing a propagating double layer which is time independent in the moving frame of reference. Under the assumption that h, v, and φ are functions of the coordinate $\xi=x-Mt$ only, (1) and (2) give

$$v=M-(M-v_0)[1-2\varphi/(M-v_0)^2]^{1/2}, \tag{4}$$

$$h=[1-2\varphi/(M-v_0)^2]^{-1/2}. \tag{5}$$

Here the "Mach number" M is the ratio between the shock velocity and $(k_B T_e/m_i)^{1/2}$. The boundary conditions have been chosen so that $h=1$ and

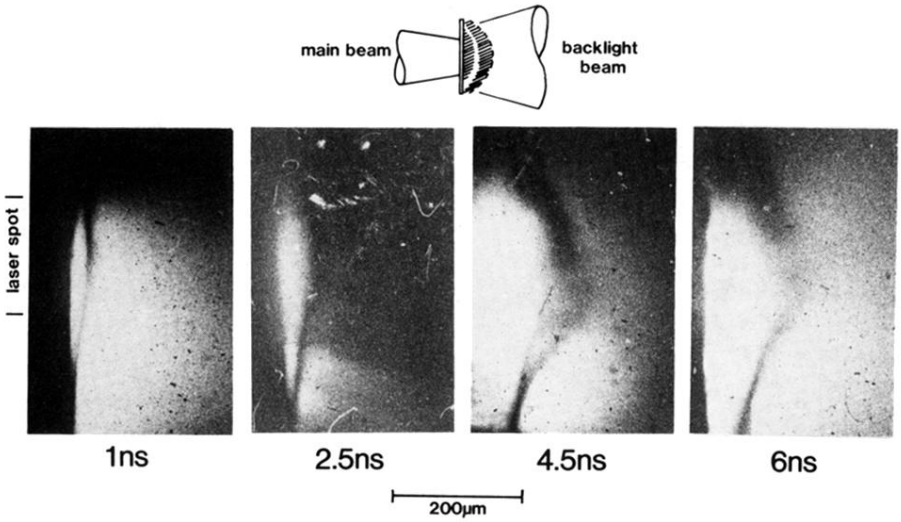

FIG. 1. Framing x-ray shadowgraphs of a 3-μm-thick Mylar foil irradiated at 3.6×10^{13} W/cm^2. The time delay between the peak of the main and backlighting pulses is shown below each image.